

## Chaotic Fluctuations and Formation of a Current Filament in $n$ -type GaAs

A. Brandl and W. Prettl

*Institut für Angewandte Physik, Universität Regensburg, D-8400 Regensburg, Federal Republic of Germany*

(Received 27 November 1990)

A novel nonlinear model is presented for the occurrence of current fluctuations at low temperatures in extrinsic semiconductors. It is based on impact ionization of shallow impurities and structure-forming processes leading to a current filament. Numerical investigations reproduce the current-voltage characteristics and reveal regular, quasiperiodic, and frequency-locked spontaneous current oscillations and a Ruelle-Takens-Newhouse transition to chaos in agreement with experimental observations in  $n$ -type GaAs.

PACS numbers: 72.20.-i, 05.40.+j, 72.70.+m

Autonomous current oscillations and chaotic fluctuations were observed in various high-purity semiconductors in the course of impurity breakdown at low temperatures.<sup>1-3</sup> Detailed experimental investigations of  $n$ -type GaAs epitaxial layers have shown that the oscillations and the nonlinearities in the current-voltage characteristics are intimately connected to the formation of a current filament<sup>4</sup> and depend on the strength of an external magnetic field.<sup>5,6</sup> Without a magnetic field only regular relaxation oscillations and stable filamentary current flow in the post-breakdown regime are observed. Applying a magnetic field significantly changes the temporal structure of oscillations and destabilizes the current filament. A second oscillatory mode spontaneously evolves which, with increasing magnetic-field strength, generates a sequence of quasiperiodic and mode-locked states. Finally, a third mode drives the system into chaos following a Ruelle-Takens-Newhouse (RTN) scenario. Several models have been developed to explain self-sustained oscillatory effects in semiconductors.<sup>7-10</sup> However, up to now the physical origin of complex current fluctuations formed by different modes of oscillations giving rise to chaos by a RTN transition is not well understood. In fact, to our knowledge no theory exists which yields a RTN scenario in an extrinsic semiconductor.

In this Letter we report on a novel nonlinear model which for the first time reproduces the dynamical phenomena observed in  $n$ -type GaAs epitaxial layers. In particular, the steady-state properties, the formation of a current filament, regular oscillations, and quasiperiodic and mode-locked current fluctuations are simulated as functions of external electric and magnetic fields in almost quantitative agreement with the experimental results. This model describes the fundamental physical reasons for a RTN transition to chaos.

Inhomogeneous current distribution in a nonequilibrium dynamical state may be described by partial differential equations which, however, are not practical to model filament formation. Based on assumptions arising from the experimentally observed spatial structure of

the current flow in a thin epitaxial layer,<sup>5</sup> the problem may be reduced to a set of coupled nonlinear ordinary differential equations which can be solved numerically. The current filament is approximated by five different zones representing the filament, the filament borders as transition zones to the high-Ohmic cladding regions, and the high-Ohmic outside zones themselves. Each zone is assumed to be homogeneous with the free-electron concentration depending only on time. The local kinetics in each zone is described by generation of free carriers due to impact ionization of shallow donors out of the ground state and one representative excited state and recombination across the excited state. This approach is in accord with the giant trap theory<sup>11</sup> and yields  $S$ -type local current-density-electric-field relations.<sup>12</sup> The interaction between the zones is mediated by lateral carrier diffusion and structure-forming processes, in particular, pinching of the filamentary current flow. These processes act as pressures on the zone interfaces<sup>13</sup> and yield dynamical variations of the zone widths and thus the current through the sample. Applying a magnetic field perpendicular to the layer and to the current accumulates space charges in the transition zones and generates a Hall field across the filament. The impact-ionization probability in the positively and negatively charged transition zones becomes higher and smaller, respectively.<sup>5</sup> This is the most important effect of the magnetic field on the filamentary current flow<sup>6</sup> which is taken into account by a corresponding increase and decrease of the driving electric fields in the borders proportional to the Hall field.

The rate equations describing the time dependence of the free-electron concentration  $n$  and the occupations of the donor ground state  $n_D$  and the excited state  $n_D^*$  are

$$\begin{aligned}\dot{n} &= X_{\uparrow}^S n_D^* + X_{\uparrow}^* n_D^* n + X_{\downarrow} n_D n - T_{\downarrow}^S p_D n, \\ \dot{n}_D^* &= T_{\downarrow}^S p_D n + X_{\downarrow}^* n_D - X_{\downarrow}^S n_D^* - X_{\uparrow}^* n_D^* n - T^* n_D^*, \\ \dot{n}_D &= T^* n_D^* - X_{\downarrow}^* n_D - X_{\downarrow} n_D n,\end{aligned}$$

where  $p_D$  is the density of ionized donors which, in the case of local neutrality, is given by  $p_D = N_A + n$ , with  $N_A$

the concentration of compensating acceptors. The impact-ionization probabilities per electron, as functions of the electric field  $E$ ,  $X_1^*(E)$  and  $X_1(E)$ , are proportional to  $\exp[-(c/E)^a]$ , with  $a$  between 1 and 2.<sup>14</sup> Single-electron processes taken into account are thermal excitation ( $X^*$ ) and thermal ionization ( $X_1^S$ ) of the excited state, capture of carriers in the excited state ( $T_1^S$ ), and relaxation to the ground state ( $T^*$ ). Thermal ionization out of the ground state may be ignored due to the low temperatures.

The high-conducting phase formed by a huge concentration of free electrons, constituting the current filament, can be regarded as a compensated nonequilibrium plasma with the restriction of immobile positive charges.<sup>15</sup> The pattern of a filamentary current flow stems from several compensating pressures on the interfaces of the zones.<sup>13</sup> Diffusion of free carriers due to the gradient in the concentration at the filament border acts as a pressure  $P_{diff} \sim n$  with a tendency of spreading the filament width. Another tendency to widen the filament derives by Ohmic heating of the filament with dissipation of electric power. This pressure  $P_{out} \sim nk_B T_e$  is proportional to the free-carrier concentration  $n$  and the free-electron temperature  $T_e$ .<sup>16</sup> Pinching,  $P_{in} \sim I_F$ , tending to shrink the current filament, with  $I_F$  the current through the filament, results from self-acting forces on the free carriers deflecting their trajectories to the center of the filament. Generally, this tendency of pinching is always present on drifting carriers.<sup>15</sup> However, the current filament is not pinched off totally because in compensated  $n$ -type semiconductors the remaining ionized positively charged donors, being fixed in space, will form space-charge regions at the filament borders giving rise to compensating counteracting electric fields limiting the pinching.<sup>15</sup> This pressure is denoted as  $P_{comp} \sim I_F$  here.

The structure-forming tendencies  $P$  and the widths  $w$  of the charged zones are sketched in Fig. 1 in a schematic drawing of the filament cross section. The five different zones are characterized by different widths, different concentrations of free carriers, different occupations of shallow impurities, and, most significant, if a magnetic field is applied, different local electrical-field strengths causing different ionization probabilities.

In order to compare the numerical results directly to those observed, the electric circuitry of the experimental setup and the dimensions of the sample have to be taken into account. The series combination of a load resistor  $R_L = 100$  k $\Omega$  and the sample, over which the voltage  $V_0$  is applied, determines the voltage  $V$  across the sample and hence the electric-field strength  $E$ . Capacitive effects and displacement currents in the sample can be regarded as a capacitance  $C$  parallel to the sample. The time dependence of the electrical field  $E$  is expressed by  $\dot{E} = (I_L - I_S)/CD$ , where  $D$  is the distance between the electrical contacts and  $I_L$  and  $I_S$  denote the current through  $R_L$  and the sample, respectively. The mobility  $\mu$

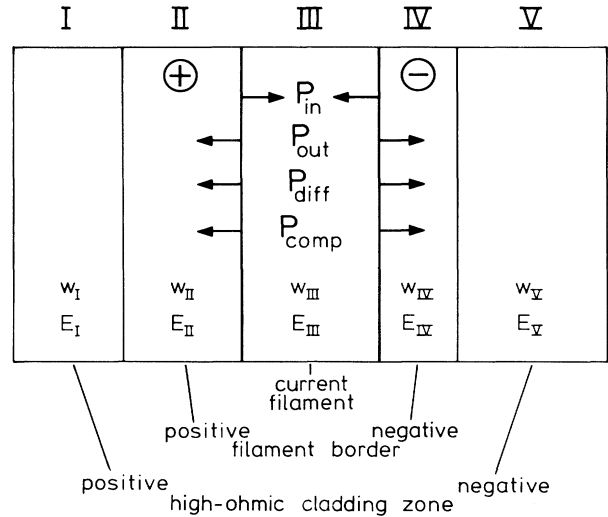


FIG. 1. Schematic cross section of a current filament in an epitaxial semiconductor layer. The structure-forming tendencies  $P$  are sketched in the five-zone model. Local electric fields  $E$  and zone widths  $w$  are dynamical variables.

of free electrons is a function of the applied magnetic-field strength  $B$  perpendicular to the current<sup>17</sup> which can be estimated as  $\mu = \mu_0/[1 + (aB)^2]$ .

The lateral distribution of free-carrier concentration is obtained by numerical calculations on five parallel working computers (INMOS T800), representing the five different zones in the sample. Each computer solves the local rate equations with regard to the zone-specific electric-field strengths. The pressures are calculated and the free-carrier concentrations of the different zones are combined to determine the total electric current  $\mu d \sum n_i E_i w_i$ , where the sum runs over the five zones and  $d$  is the thickness of the sample. Then the voltage across the sample and the local electric fields for the different zones, taking into account the Hall field, are determined. Finally, the filament width and the lateral extensions of the zones are adjusted from the pressure imbalance at the interfaces. Successive calculation of the above described procedure will reveal the temporal behavior in the current and the spatiotemporal structure of the current filament.

The simulation was performed with the material parameters of the sample investigated in the experiment of Ref. 6. Together with  $C = 9.6$  pF,  $a = 17$  m<sup>2</sup>/V s, and  $\mu_0 = 4 \times 10^4$  cm<sup>2</sup>/V s for the electron mobility at 4.2 K, the best numerical fit has been obtained with  $\alpha = 2$ , impact-ionization coefficients  $X_1^*(\infty) = 4.4 \times 10^{-5}$  cm<sup>3</sup>/s and  $X_1(\infty) = 2.2 \times 10^{-5}$  cm<sup>3</sup>/s, and  $c = 1.22$  and 2.44 V/cm for the excited and ground states of the donors, respectively. The remaining coefficients are  $T_1^S = 4.5 \times 10^{-6}$  cm<sup>3</sup>/s,  $T^* = 4.1 \times 10^7$  s<sup>-1</sup>,  $X_1^S = 1.17 \times 10^6$  s<sup>-1</sup>, and  $X^* = 2.34 \times 10^6$  s<sup>-1</sup>. The order of magnitude of the kinetic parameters fits in well with previous investiga-

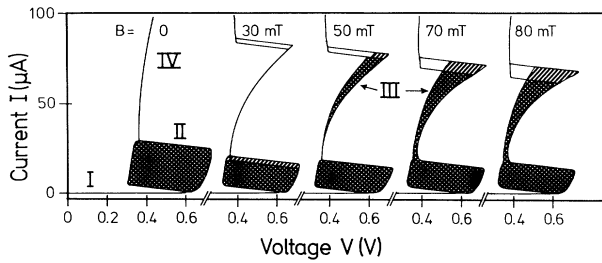


FIG. 2. Calculated current-voltage characteristics for various magnetic fields  $B$  (load resistor  $R_L = 1 \text{ M}\Omega$  and bath temperature  $T = 4.2 \text{ K}$ ). Regions of distinct characteristic oscillations I-IV are indicated (see text). The extent of the oscillatory regime is marked by hatching (hatching inclined from bottom left to top right denotes recording direction to increasing current; that from top left to bottom right denotes decreasing current).

tions.<sup>18</sup> Figure 2 shows calculated current-voltage characteristics for different magnetic-field strengths in good agreement with experimental results.<sup>3,6</sup> The characteristic regimes of distinct current behavior are almost quantitatively reproduced: (I) stable high-impedance current flow, (II) large-amplitude relaxation oscillations with frequencies up to 5 MHz, (III) small-amplitude fluctuations of complex temporal behavior for  $B \neq 0$ , and (IV) stable low-impedance current post-breakdown behavior. Numerical solutions are shown in Figs. 3 and 4 in comparison with the experimental results. The temporal characteristics of the large-amplitude relaxation oscillation are shown in Fig. 3(a) for two different bias voltages  $V_0$ . These relaxation oscillations are the result of repetitive ignition and extinction of an impact-ionization avalanche yielding a flashing current filament. At sufficiently large average currents a filament is formed which is stable for  $B = 0$ . For  $B > 30 \text{ mT}$  and in regime III, where a current filament is formed and the structure-forming tendencies are important, different modes of oscillation arise. One fundamental current oscillation derives from the cyclic ignition and extinction of the local impact-ionization breakdown inside the positively charged filament border. A second mode stems from the fluctuations in the concentration of free carriers inside the current filament due to fluctuations in  $E$ . As a consequence of the structure-forming tendencies, the widths of the filament and of the charged zones oscillate. At small magnetic fields where coupling between these two modes is weak, quasiperiodic behavior is obtained, as shown in Fig. 3(b). At increased magnetic-field strengths the electric Hall field and the width of the positive transition zone are enlarged and hence the current flow is destabilized in a more drastic way. This can be regarded as an increased coupling strength between the two different oscillating modes. Thus, mode locking occurs as predicted by the circle-map theory.<sup>19</sup> The temporal characteristics in the mode-locking regime are

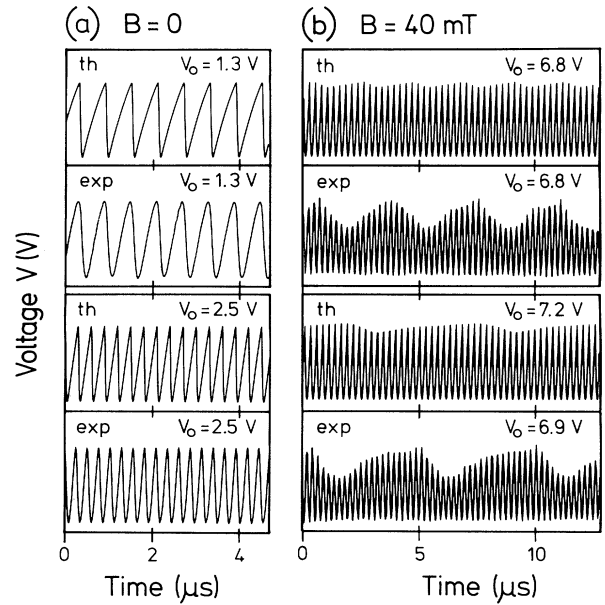


FIG. 3. Temporal structure of voltage oscillations for different magnetic fields  $B$  and two different bias voltages  $V_0$  each. Theoretical and experimental curves are indicated by "th" and "exp," respectively. (a) Regular oscillations in regime II at  $B = 0$  and (b) quasiperiodic oscillations in regime III at  $B = 40 \text{ mT}$ .

shown in Fig. 4. The width of the positively charged zone at the current filament border reveals a high-frequency mode of oscillation, whereas the low-frequency mode is defined by repetitively occurring large excursions in the width or breathing of the current filament. Another mode of destabilization is introduced for magnetic fields and electrical-field strengths high enough to surpass the impact-ionization threshold in the negatively charged zone. This will lead to a collapse in the Hall voltage.<sup>6</sup> In combination with the former two modes of oscillation, the semiconductor exhibits chaotic current

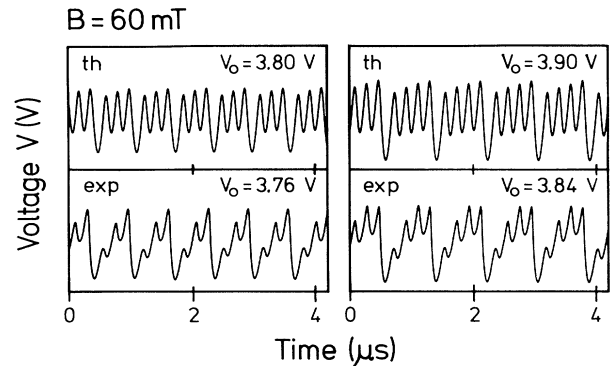


FIG. 4. Temporal structure of mode-locked voltage oscillations for  $B = 60 \text{ mT}$ . The frequency ratios  $\frac{1}{3}$  and  $\frac{1}{4}$  are plotted; "th" and "exp" denote calculated and measured curves.

fluctuations. Thus, a RTN transition to chaos can be described by this five-zone, three-level model. For higher currents the pinching tendency dominates over the destabilizing processes, forcing a stable current filament monotonously increasing in width as a function of the current.

In summary, an explanation of the temporal structure of nonlinear current fluctuations in thin extrinsic semiconductor layers, the formation and the spatiotemporal behavior of a current filament, and the overall current-voltage characteristics can be given by the above described model as a function of external control parameters. The essential approach suggested by experimental results is the division of the sample into five different spatial zones characterized by local electrical fields. Structure-forming processes are taken into account by pressures on the interfaces between the zones derived from free-carrier concentrations. The number of free carriers in each zone is determined by standard nonlinear generation-recombination kinetics.

We thank E. Bauser, Max-Planck-Institut für Festkörperforschung, Stuttgart, for provision of the sample and G. Obermair, E. Schöll, and R. P. Huebener for helpful discussions. Financial support by the Deutsche Forschungsgemeinschaft is gratefully acknowledged.

---

<sup>1</sup>S. W. Teitsworth, R. M. Westervelt, and E. E. Haller, Phys. Rev. Lett. **51**, 825 (1983); G. A. Held, C. Jeffries, and E. E. Haller, Phys. Rev. Lett. **52**, 1037 (1984); D. G. Seiler, C. L. Littler, R. J. Justice, and P. W. Milonni, Phys. Lett. A **108**, 462 (1985); J. Peinke, J. Parisi, B. Röhrich, K. M. Mayer, U. Rau, and R. P. Huebener, Solid State Electron. **31**, 817 (1988); K. Aoki and K. Yamamoto, Appl. Phys. A **48**, 111 (1989).

<sup>2</sup>A. Brandl, T. Geisel, and W. Prettl, Europhys. Lett. **3**, 401 (1987).

<sup>3</sup>J. Spangler, A. Brandl, and W. Prettl, Appl. Phys. A **48**, 143 (1989); U. Frank, A. Brandl, and W. Prettl, Solid State Commun. **69**, 891 (1989).

<sup>4</sup>A. Brandl, M. Völcker, and W. Prettl, Solid State Com-

mun. **72**, 847 (1989).

<sup>5</sup>A. Brandl, M. Völcker, and W. Prettl, Appl. Phys. Lett. **55**, 238 (1989).

<sup>6</sup>A. Brandl, W. Kröniger, W. Prettl, and G. Obermair, Phys. Rev. Lett. **64**, 212 (1990).

<sup>7</sup>A. G. Chynoweth and A. A. Murray, Phys. Rev. **123**, 515 (1961).

<sup>8</sup>M. Glicksman, Phys. Rev. **124**, 1655 (1961); F. C. Hoh and B. Lehnert, Phys. Rev. Lett. **7**, 75 (1961); L. E. Gurevich and I. V. Ioffe, Fiz. Tverd. Tela (Leningrad) **4**, 2641 (1963); **4**, 2964 (1963); **6**, 445 (1964) [Sov. Phys. Solid State **4**, 1938 (1963); **4**, 2173 (1963); **6**, 354 (1964)]; C. E. Hurwitz and A. L. McWorther, Phys. Rev. **134**, A1033 (1964); R. M. Westervelt and S. W. Teitsworth, J. Appl. Phys. **57**, 5457 (1985); C. D. Jeffries, Phys. Scr. **T9**, 11 (1985).

<sup>9</sup>K. A. Piragas, Fiz. Tekh. Poluprovodn. **17**, 1035 (1983) [Sov. Phys. Semicond. **17**, 652 (1983)].

<sup>10</sup>V. L. Bronch-Bruevich and S. G. Kalashnikov, Fiz. Tverd. Tela (Leningrad) **7**, 750 (1965) [Sov. Phys. Solid State **7**, 599 (1965)]; E. Schöll, Phys. Rev. B **34**, 1395 (1986); E. Schöll, *Nonequilibrium Phase Transitions in Semiconductors* (Springer, Berlin, Heidelberg, 1987), 1st ed.

<sup>11</sup>M. Lax, J. Phys. Chem. Solids **8**, 66 (1959).

<sup>12</sup>E. Schöll, Z. Phys. B **46**, 23 (1982); Appl. Phys. A **48**, 95 (1989).

<sup>13</sup>J. Pozhela, *Plasma and Current Instabilities in Semiconductors* (Pergamon, Oxford, 1981).

<sup>14</sup>G. A. Baraff, Phys. Rev. **128**, 2507 (1962).

<sup>15</sup>M. Glicksman, in *Plasma Effects in Solids*, Proceedings of the Seventh International Conference on the Physics of Semiconductors, edited by J. Bok (Dunod, Paris, 1965), Vol. 2, p. 149ff; B. Ancker-Johnson, *Semiconductors and Semimetals* (Academic, New York, 1966), Vol. 1, p. 379.

<sup>16</sup>B. D. Osipov and A. N. Khvoshchev, Zh. Eksp. Teor. Fiz. **43**, 1179 (1963) [Sov. Phys. JETP **16**, 833 (1963)]; F. F. Chen, *Introduction to Plasma Physics* (Plenum, New York, 1974).

<sup>17</sup>W. Schneider, Appl. Phys. **11**, 141 (1976).

<sup>18</sup>V. N. Zverev and D. V. Skovkun, Zh. Eksp. Teor. Fiz. **87**, 1745 (1984) [Sov. Phys. JETP **60**, 1003 (1984)]; M. Weispfenning, I. Hoeser, W. Böhm, and W. Prettl, Phys. Rev. Lett. **55**, 754 (1985); J. Kaminski, J. Spector, W. Prettl, and M. Weispfenning, Appl. Phys. Lett. **52**, 233 (1985).

<sup>19</sup>M. H. Jensen, P. Bak, and T. Bohr, Phys. Rev. A **30**, 1960 (1984); **30**, 1970 (1984).